THE ASTROPHYSICAL JOURNAL, 377:L29–L32, 1991 August 10

FIRST RESULTS FROM THE GODDARD HIGH-RESOLUTION SPECTROGRAPH: SPECTROSCOPIC DETERMINATION OF STELLAR PARAMETERS OF MELNICK 42, AN O3f STAR IN THE LARGE MAGELLANIC CLOUD

S. R. HEAP,[1,2] B. ALTNER,[2,3] D. EBBETS,[1,4] I. HUBENY,[2,5] J. B. HUTCHINGS,[1,6] R. P. KUDRITZKI,[7,8]
S. A. VOELS,[7] S. HASER,[7,8] A. PAULDRACH,[7] J. PULS,[7] AND K. BUTLER[7]
Received 1991 March 29; accepted 1991 May 7

ABSTRACT

GHRS and optical (ESO 3.6 m) observations of the O3f star Melnick 42 in the 30 Doradus complex are reported. A first analysis reveals that with a luminosity of $2.3 \times 10^6\ L_\odot$ and a present mass of $100\ M_\odot$, Melnick 42 is one of the most luminous and massive stars known. An estimate of abundances indicates that iron and oxygen are very likely reduced by a factor of 4 relative to the Sun, whereas carbon is more strongly depleted and nitrogen is approximately solar. The terminal velocity of the stellar wind is 3000 km s^{-1}. The mass-loss rate is $4 \times 10^{-6}\ M_\odot\ yr^{-1}$, with a large uncertainty.

The excellent quality GHRS spectrum taken in a crowded region of the LMC demonstrates the superiority of the *HST* for quantitative ultraviolet spectroscopy of hot stars in other galaxies.

Subject headings: galaxies: Magellanic Clouds — stars: individual (Melnick 42) — stars: massive — stars: Of-type — stars: winds — ultraviolet: spectra

1. INTRODUCTION

We report on observations made with the Goddard High-Resolution Spectrograph (GHRS) of Melnick 42 (Brey 77), a very hot, massive star in the 30 Doradus complex in the Large Magellanic Cloud (LMC; Melnick 1985). Our objectives were (1) to evaluate the capabilities of the GHRS for crowded-field, faint-object spectroscopy and (2) to investigate the possibility of deriving the basic parameters of a hot star purely from spectroscopic data. Melnick 42 is well suited for both purposes. Since the star lies in the LMC, its distance is well known ($m - M = 18.57$; Panagia 1991), and so the spectroscopically derived parameters can be verified. Since the LMC has a low metal content relative to the Galaxy (Dufour 1984; Barlow 1990; Dopita 1990), we can learn how chemical composition affects the wind velocity and rate of mass loss from this star.

In this *Letter*, we report on the first observational results regarding the basic parameters of the star and its wind. We leave to a later paper the full theoretical interpretation of the observations. In §§ 2 and 3, we describe the ultraviolet and optical spectrum of Melnick 42. In § 4, we describe our analyses of the UV wind spectrum, with a summary in § 5.

2. OBSERVATIONS AND DATA REDUCTION

The operation of the GHRS is fully described in the "GHRS Handbook V2.0" by Ebbets & Duncan (1989). We first obtained two series of FP-SPLIT spectra using the G140L grating with the star centered in the Large Science Aperture (2″; LSA). One series covered the spectral region 1150–1450 Å and the other, 1490–1750 Å. The star was then slewed to the Small Science Aperture (0.″2; SSA), and the observations were repeated. The short-wavelength SSA spectra took 29 minutes, while the long-wavelength spectra took 116 minutes. The FP-SPLIT option provides a series of spectra at four different grating positions. To combine these exposures, we estimated the wavelength offset of each spectrum with respect to the first by cross-correlating interstellar lines, shifting the spectrum by the appropriate amount, and co-adding. We applied dispersion constants derived from spectra of the internal platinum lamp, taken immediately before observations of Melnick 42, to obtain heliocentric wavelengths for each data point. Most interstellar lines are resolved in the SSA spectrum into Galactic and LMC components, which on average, are at radial velocities of +56 km s^{-1} and +257 km s^{-1}, respectively. The radial velocity of the photospheric spectrum is +261 km s^{-1}, based on a comparison of a spectral region containing many Fe and Ni lines (1350–1450 Å) with a synthetic spectrum. We therefore adjusted the wavelength scale by 261 km s^{-1} to put the spectrum in the rest frame of the star.

We compared the LSA and SSA spectra of Melnick 42 with respect to efficiency, spectral resolution, and line profile accuracy. We found that due to spherical aberration and spacecraft jitter, the throughput of the SSA is considerably lower than that of the LSA: by a factor of 5.0 at λ1150, 4.5 at Lyα, and 4.0 at C IV 1550. However, SSA spectra are *not* degraded by a loss of spectral purity; they achieve the full instrumental resolution (0.6 Å for grating G140L). We deconvolved the LSA spectrum using a line-spread function derived from ultraviolet FOC pictures of isolated stars. Although we tried several different methods (cf. Lindler 1990), all of which gave similar results, we could not reproduce the depth of the absorption components of saturated wind features seen in the SSA spectrum. We attribute this difference to continuous emission from faint neighboring stars within the LSA, which are masked out by the SSA.

For scientific purposes we therefore worked only with the normalized SSA spectra. We found that we could best estimate the continuum level after applying an absolute flux calibration (based on observations of the standard star, BD +75°325) and

[1] Goddard High Resolution Spectrograph (GHRS) Investigation Definition Team.
[2] Goddard Space Flight Center, Code 681, Greenbelt, MD 20771.
[3] Astronomy Programs, Computer Sciences Corporation.
[4] Ball Aerospace Systems Division, P.O. Box 1062, JWF-3, Boulder, CO 80306.
[5] Universities Space Research Association (USRA).
[6] Dominion Astrophysical Observatory, 5071 West Saanich Road, Victoria, BC, Canada V8X 4M6.
[7] Institut für Astronomie und Astrophysik der Universität München, Scheinerstrasse 1, 8000 Munich 80, Germany.
[8] Max-Planck-Institut für Astrophysik, Garching bei München.

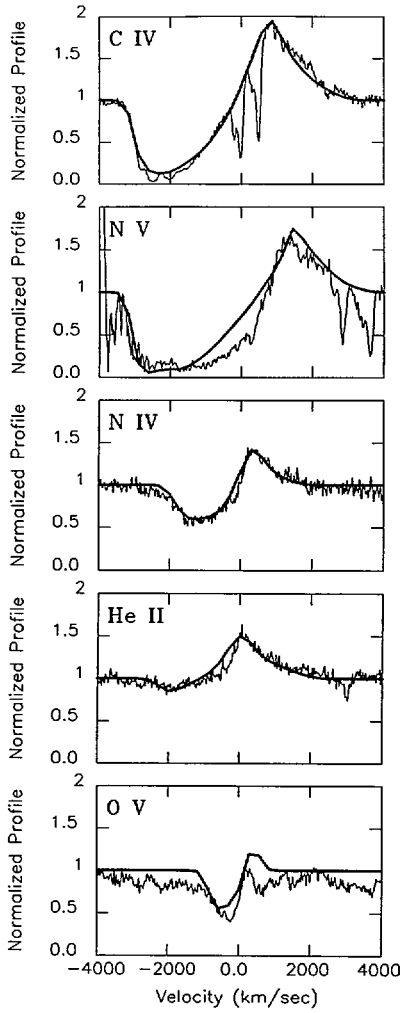

FIG. 1.—UV wind lines in Melnick 42. Each panel shows the normalized P Cygni profiles (*thin solid line*) and the best fit (*heavy solid line*). The N v λ1240 line was corrected for extinction by interstellar Lyα. The O v λ1370 line fit assumed strong photospheric absorption. the He II λ1640 line required a very large collisional term in the source function and could not be used to estimate the mass loss rate.

dereddening the spectrum (cf. § 3). In addition, we corrected the wind line profile of N v λ1240 for extinction by Lyα, using $N_{\rm col}({\rm gal}) = 1 \times 10^{21}$ cm^{-2} and $N_{\rm col}({\rm LMC}) = 5 \times 10^{21}$ cm^{-2}. Figure 1 shows the resultant normalized profiles of the major wind features. The high signal-to-noise of the GHRS spectra (estimated at 20 for N v λ1240 and 34 at C IV λ1550) provides a precise definition of these wind line profiles. Note that the C IV wind feature shows narrow, high-velocity ($0.83v_\infty$) absorption in each doublet component.

3. LUMINOSITY AND ANALYSIS OF THE OPTICAL SPECTRUM

Spectrograms of Melnick 42 were first obtained by Melnick (1985) at the European Southern Observatory (ESO). He classified the spectrum as O3f, based on the absence of stellar He I λ4471. In parallel with the GHRS observations, optical spectra were obtained by one of us (S. V.) with the ESO 3.6 m telescope and its Cassegrain echelle spectrograph (CASPEC). These high-dispersion echellograms reveal that He I λ4471 is indeed present, although it is weak and partially obscured by nebular emission. From this line and profiles of Hγ and He II λ4542, we derive the stellar parameters: $T_{\rm eff} = 42{,}500 \pm 2000$ K, $\log g = 3.5 \pm 0.15$, $N({\rm He})/N({\rm H}) = 0.10$–$0.15$, and $v_{\rm rot} = 200$–250 km s^{-1}, using NLTE model photospheres.

CCD photometry of the 30 Doradus region by J. Parker (1990, private communication) gives $V = 12.64$, $B-V = 0.06$, and $U-B = 0.84$ for Melnick 42. Taking a LMC distance modulus of $m - M = 18.57$ (Panagia 1991) and $V_0 = 11.40$, we derive a stellar radius of $R = 28\ R_\odot$ (see Kudritzki 1980). The bolometric luminosity is then $L_{\rm bol} = 2.3(\pm 0.4) \times 10^6\ L_\odot$, where the quoted errors correspond to uncertainties in $T_{\rm eff}$ only. We also derived the luminosity by comparing the reddening-corrected UV and visible continuum to models with the above $T_{\rm eff}$. We obtain a best fit for a foreground color excess $E(B-V) = 0.06$, and LMC halo $E(B-V) = 0.04$, a 30 Dor region $E(B-V) = 0.10$ (E. L. Fitzpatrick, private comminication), and a 30 Dor central region $E(B-V) = 0.20$. Except for the 30 Dor region, which has a unique extinction law (Fitzpatrick 1985), the extinction is of a "Galactic type" in the UV (Savage & Mathis 1981; Fitzpatrick & Savage 1984). This continuum fit yields a $L_{\rm bol} = 2.5 \times 10^6\ L_\odot$. When compared to Maeder's (1990) evolutionary tracks for stars of low metallicity ($Z = 0.005$), the $T_{\rm eff}$ and $L_{\rm bol}$ of Melnick 42 suggest a ZAMS mass of 120 $M_\odot$ and a present-day stellar mass of $M_{\rm ev} = 110\ M_\odot$. The mass derived from the spectroscopic gravity and the radius is $M_{\rm gr} = 90(+37, -26)\ M_\odot$.

4. ANALYSIS OF THE WIND SPECTRUM

The GHRS spectrum is dominated by features formed in the wind of Melnick 42 (see Figs. 2 and 3). Identifiable P Cygni lines include N v λ1240, O v λ1370, C IV λ1549, He II λ1640, and N IV λ1718. Both the Goddard and Munich groups independently fitted these lines with model profiles calculated in a manner similar to that described by Lamers, Cerruti-Sola, & Perinotto (1987), with results as shown in Figure 1. Although we show the fits to all of these lines in Figure 1, we concentrate only on the C IV and N v lines in this *Letter*. We obtain $v_\infty = 3000$ km s^{-1} and $\beta = 0.7$–1.0, parameters in the wind velocity law $v(r) \approx v_\infty(1 - R_*/r)^\beta$. For most wind lines, a simplified opacity law suffices: $\tau(w) \sim w^\gamma$, where $w = v(r)/v_\infty$. We obtain $\gamma = -0.3$ for C IV and -2.5 for N IV. For N v, a more complex opacity law is needed, and even then the fit is not as good as for the other lines.

The line fits contain information about the stellar mass-loss if the ionization fractions, $q = N_{\rm ion}/N_{\rm el}$, and abundances can be determined. To estimate q we found it necessary to integrate over the theoretical ionization stratification rather than taking q at one specific point in the wind (e.g., at $w = 0.5$) and applying it throughout, as is usually done. In this way we obtain a mass-loss rate from the N v and C IV resonance doublets:

$$\log \dot{M} + [{\rm C}] = -6.7 \pm 0.2\ , \qquad (1)$$

$$\log \dot{M} + [{\rm N}] = -5.3 \pm 0.4\ , \qquad (2)$$

where [C] is the logarithmic abundance of carbon relative to solar, and likewise for [N]. Since the surface abundance of Melnick 42 may have already been altered by nuclear-processed material brought up to the surface, we let $[{\rm X}] = [{\rm X}]_{\rm ZAMS} + [\Delta{\rm X}]_{\rm ev}$, where $[{\rm X}]_{\rm ZAMS}$ is the initial abundance and $[\Delta{\rm X}]_{\rm ev}$ is the logarithmic change induced during stellar evolution. Maeder's (1990) models for stars of low metallicity ($Z = 0.005$) suggest that the surface carbon abundance will decrease with time as the nitrogen increases, viz:

$$[\Delta{\rm C}]_{\rm ev} = -0.13[\Delta{\rm N}]_{\rm ev} \quad \text{for} \quad [\Delta{\rm N}]_{\rm ev} < 0.6 \qquad (3)$$

$$= 0.27 - 0.58[\Delta{\rm N}]_{\rm ev} \quad \text{for} \quad [\Delta{\rm N}]_{\rm ev} \geq 0.6\ , \qquad (4)$$

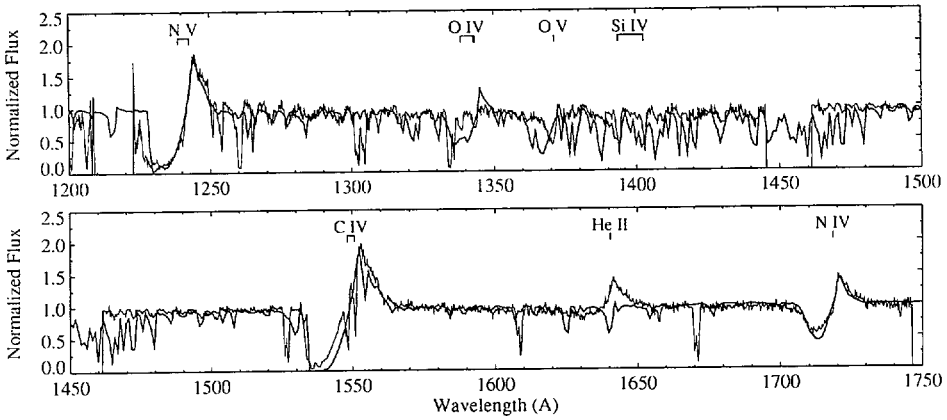

FIG. 2.—Comparison of a model wind spectrum computed for solar abundances and the observed (normalized) spectrum of Melnick 42

provided there is no large increase in helium abundance. Taking as a first guess $[N]_{ZAMS} = -1.0$ and $[C]_{ZAMS} = -0.7$ (as inferred from observations of LMC H II regions), we obtain $\dot{M} \approx 3 \times 10^{-6}\ M_\odot\ \mathrm{yr}^{-1}$ (with a factor of 3 uncertainty), a nitrogen overabundance factor of 1.6 with respect to solar, and a carbon underabundance factor of approximately 15.

A more accurate determination of mass-loss rate and abundances requires a more elaborate analysis. We report here the first results. Figure 2 compares the full GHRS spectrum of Melnick 42 compared with the spectrum of a self-consistent, NLTE, hydrodynamical, radiation-driven wind model calculated for $T_{\mathrm{eff}} = 42{,}500$ K, $\log g = 3.55$, $R = 26\ R_\odot$, and solar abundances. The mass-loss rate of the model is $7.6 \times 10^{-6}\ M_\odot\ \mathrm{yr}^{-1}$ and v_∞ is 2300 km s^{-1}. (For the physics of the models, see Pauldrach et al. 1990 and references therein.) The comparison implies that carbon and oxygen must be underabundant, whereas a solar abundance for nitrogen might be in order, and most strikingly, iron (which produces much of the absorption between 1370 and 1480 Å) is underabundant. Figure 3 compares the observations with a theoretical model computed with most metal abundances reduced by a factor of 4 relative to solar; the exceptions are nitrogen with solar abundance and carbon reduced to one-twentieth of solar. The mass-loss rate of the model is $4.1 \times 10^{-6}\ M_\odot\ \mathrm{yr}^{-1}$ and v_∞ is 2900 km s^{-1}, in agreement with the results from the wind-line fitting in § 3. The fits of N IV, N V, C IV, and O V are reasonable; Si IV is probably contaminated by photospheric and/or interstellar contributions. The Fe V features are now a bit weaker than observed, but this is most likely due to the fact that the model does not include a photospheric contribution (cf. Hubeny, Heap, & Altner 1991). The only striking discrepancy in Figures 2 and 3 is the He II λ1640 line. This line, together with He II λ4686 and Hα emission in the optical spectra, indicates higher opacity in these lines than produced by the models. This discrepancy is presently under investigation.

These self-consistent calculations illustrate the complex interdependence of metallicity and the properties of the wind. A change in metallicity affects the optical thickness in the He II continuum and therefore the ionization state of the wind. The changed ionization in turn affects the acceleration of the wind and can compensate for a lower metallicity. For SMC stars, metallicity effects normally dominate ionization effects. However, in the LMC star Melnick 42, ionization effects apparently dominate. Thus, lowering the metallicity by a factor of 4 results in an *increase* in v_∞ from 2300 to 2900 km s^{-1} (cf. Fig. 2 vs. Fig. 3).

Kudritzki & Hummer (1990) have shown that the mass-loss parameters, v_∞ and $\dot{M}$, can be used to determine stellar masses and radii. We therefore calculated v_∞ and $\dot{M}$ as a function of mass and radius using the analytical approach of Kudritzki et al. (1989) and the force multiplier parameters corresponding to the model spectrum pictured in Figure 3 ($\alpha = 0.71$, $\delta = 0.058$, $k = 0.035$, $\beta = 1.0$). The result is shown in Figure 4. If we again use the distance modulus of Panagia (1991) for the LMC, which implies $R = 28 \pm 2\ R_\odot$ along with $v_\infty = 3000 \pm 100$ km s^{-1}, we derive a stellar mass, $M = 102\ (+16, -13)\ M_\odot$. For a

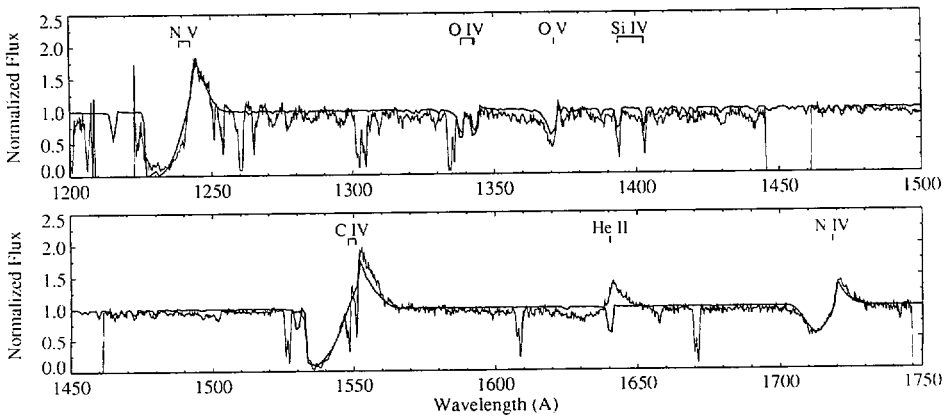

FIG. 3.—Same as Fig. 2, except that the model abundances are reduced to one-quarter solar for most elements, but solar for nitrogen and 0.05 solar for carbon

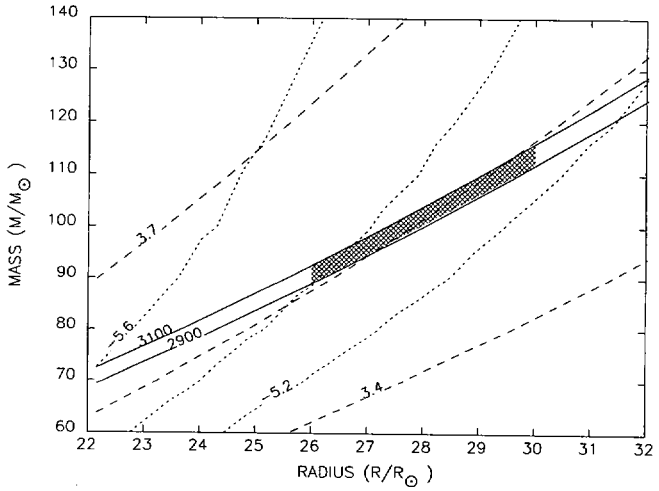

FIG. 4.—Mass-radius diagram for Melnick 42. The solid curves give the domain where the theory of radiatively driven winds reproduces the observed terminal velocity. Dotted curves indicate constant (logarithmic) mass-loss rates in solar masses per year. Dashed curves represent constant log g. The hash marks delineate the region of uncertainty in stellar radius and terminal velocity, from which we determine a mass of $M = 102(+16, -13)\ M_\odot$ (see text).

purely spectroscopic method, this is a precise determination of stellar mass, more reliable than the masses derived from evolutionary tracks or log g (see § 3). Conversely, if we adopt $\log \dot{M} = -5.4 \pm 0.2$ and the same terminal velocity, we obtain $R = 26(+6, -4)\ R_\odot$, which leads to a LMC distance modulus of $m - M = 18.5 \pm 0.5$ mag. In principle, this confirms the potential of the method. However, the mass-loss rate is too uncertain for this to be regarded as an independent determination of distance.

5. SUMMARY

First, the GHRS has obtained excellent spectra of a very massive hot star in a crowded region of the LMC—a project impossible for *IUE* because of its coarser spatial resolution and lower limiting signal-to-noise ratio. This success bodes well for future *HST* observations of OB stars in the Magellanic Clouds. Second, modern techniques of quantitative spectral analysis make possible a first determination of stellar parameters, including abundances and mass-loss rate. Because of the observed emission strengths of He II λ1640, He II λ4686, and Hα, the mass-loss rate must be regarded as uncertain. We are presently working to reduce this uncertainty. Finally, with a luminosity of $2.3 \times 10^6\ L_\odot$ and a present mass of $100\ M_\odot$, Melnick 42 is one of the most luminous and massive stars known. It is important to note that WF/PC images of the region containing Melnick 42 do not indicate any multiplicity in this object. We regard this as a convincing proof of the existence of very massive stars.

The Goddard group is grateful to Henny Lamers for providing the SEI FORTRAN code and for sage advice on its application. This work was partially supported by the Bundesministerium für Forschung and Technologie under grant 010R90080 to R. P. K.

REFERENCES

Barlow, M. J. 1990, in IAU Symposium 148, The Magellanic Clouds, ed. R. Haynes & D. Milne (Dordrecht: Kluwer), 291
Dopita, M. A. 1990, in IAU Symposium 148, The Magellanic Clouds, ed. R. Haynes & D. Milne (Dordrecht: Kluwer), 299
Dufour, R. J. 1984, in IAU Symposium 108, Structure and Evolution of the Magellanic Clouds, ed. S. van den Bergh & K. S. de Boer (Dordrecht: Reidel), 353
Ebbets, D., & Duncan, D. K. 1989, Goddard High-Resolution Spectrograph Instrument Handbook, Version 2.0, Space Telescope Science Institute
Fitzpatrick, E. L. 1985, ApJ, 299, 219
Fitzpatrick, E. L., & Savage, B. D. 1984, ApJ, 279, 578
Hubeny, I., Heap, S. R., & Altner, B. 1991, ApJ, 377, L33
Kudritzki, R. P. 1980, A&A, 85, 174
Kudritzki, R. P., & Hummer, D. G. 1990, ARA&A, 28, 303
Kudritzki, R. P., Pauldrach, A. Puls, J., & Abbott, D. C. 1989, A&A, 219, 205
Lamers, H. J. G. L. M., Cerruti-Sola, M., & Perinotto, M. 1987, ApJ, 314, 726
Lindler, D. J. 1990, in The Restoration of HST Images and Spectra, ed. R. L. White & R. Allen (Baltimore: Space Telescope Science Institute), 39
Maeder, A. 1990, A&AS, 84, 139
Melnick, J. 1985, A&A, 153, 235
Panagia, N. 1991, preprint
Pauldrach, A., Kudritzki, R. P., Puls, J., & Butler, K. 1990, A&A, 228, 125
Savage, B. D., & Mathis, J. 1981, ARA&A, 17, 73